ASIA-PACIFIC
SOLAR RESEARCH CONFERENCE

Effects of Dark Annealing in Cast-Mono Silicon

Aref Samadi[1], Carlos Vargas, Shaoyang Liu, Utkarshaa Varshney, Chandany Sen, Alison Ciesla, Catherine Chan

[1]*School of Photovoltaic and Renewable Energy Engineering, UNSW Sydney, NSW 2052, Australia*
E-mail: aref.samadi@unsw.edu.au

Cast-monocrystalline silicon is produced by a seeded casting growth method similar to multicrystalline silicon with the potential of having mono-like regions like single crystal Czochralski (Cz) grown wafers. The dislocation networks caused due to stress [1][2] and impurity variation [3] during the growth process create a non-uniform distribution of potential efficiency across ingots [4] and present a manufacturing challenge [5][6] in achieving cells with similar performance characteristics. Post-processing methods employing hydrogenation [7] provide a possibility of reducing bulk recombination in this type of material. We recently reported the improvements in carrier lifetimes observed due to dark annealing after firing on diffused samples passivated with hydrogen-rich silicon nitride (SiN_x:H) films [8]. In that work, the annealing step was done at a single temperature for a fixed duration. In this study, we vary the temperature and duration to find the optimum conditions for using dark annealing as a mechanism for improving the minority carrier lifetimes in cast-mono silicon lifetime structures.

Cast-mono *p*-type 6-inch wafers with a base resistivity of 1.5 Ω.cm were phosphorous diffused with a resulting sheet resistance of ~95 Ω/sq and symmetrically passivated with a remote plasma enhanced chemical vapour deposition (PECVD) based 75 nm SiN_x:H film (MAiA, Roth & Rau). These lifetime test structures were then fired at a peak actual temperature of 740 °C in a firing furnace (CAMiNI, Roth & Rau). The wafers were laser cleaved into 5.2 cm x 5.2 cm tokens and split into four separate groups. They were dark annealed in a controlled furnace with varied temperatures and holding times. The dark annealing temperatures were varied from 300 °C to 600 °C and the annealing times from one minute to seven minutes. The minority carrier lifetime in the samples before and after annealing was measured via quasi-steady-state photoconductance (QSSPC) measurements (WCT120, Sinton Instruments) and the spatial recombination was recorded using photoluminescence (PL) imaging (LIS-R3, BT Imaging). The outline of the experimental flow is shown in Figure 1.

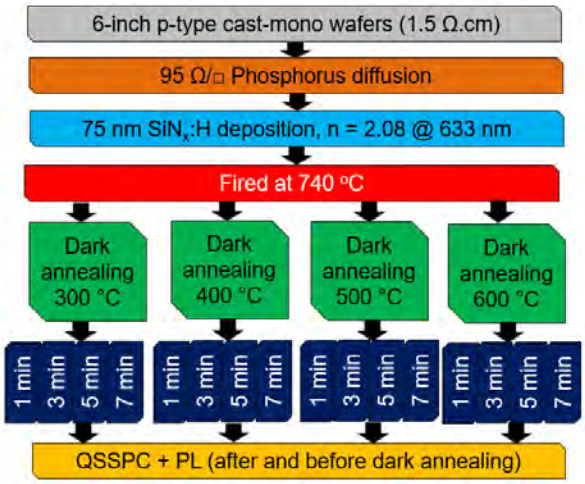

Figure 1. Experimental outline to investigate the impact of dark annealing time and temperature on cast-mono lifetime samples.

The relative changes in effective lifetimes $(\tau_{DA} - \tau_{fired})/\tau_{fired}$ are presented in Figure 2 (a). Not all the tokens are sisters and this could have an influence on the results. The average initial effective lifetime of the samples used was ~35 µs. At 300 °C, prolonged dark annealing leads to a larger improvement. The improvements appear to be located in the regions with high dislocation densities surrounding the mono-like regions, as observed in Figure 3. This is expected considering the enhanced passivating ability of hydrogen in dislocation networks [9]. Longer treatment times, however, appear to lead to degradation of the mono-like regions. At 400 °C the optimum annealing time is found to be around 3 min. It must be noted that in this set not all the tokens were complete sister and the sample at 3 min had more dislocations which could have affected the results. At 500 °C the best improvement was achieved with the shortest treatment time with a relative improvement of approximately 80%. At 600 °C a very small improvement in effective lifetime of approximately 13% was observed which was independent of the dark annealing duration, however there appeared to be a degradation in mono-like regions with treatment times above 1 min for this temperature and hence the improvements were mostly observed in the dislocated regions. The best condition for this set of samples was found to be for a dark annealing temperature of 300 °C for 7 min with a trend of larger improvements at higher treatment times. The interpolated surface map of time versus temperature is plotted in Figure 2 (b).

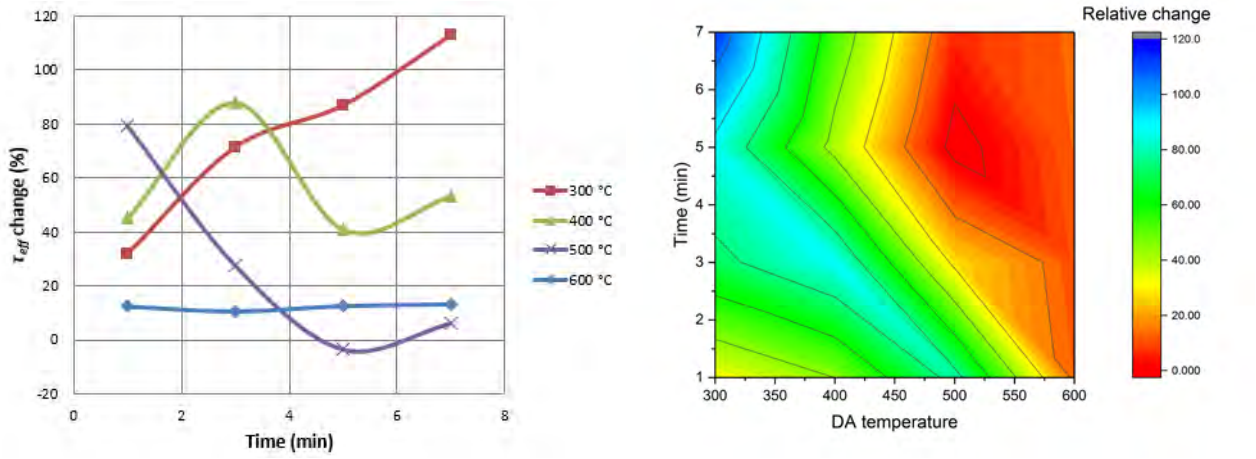

(a) (b)

Figure 2. (a) Relative change in effective lifetime before and after dark annealing at different temperatures and durations . (b) Interpolated values for the relative change in lifetime after dark annealing in a time versus temperature surface map.

The optimal point obtained in this experiment could potentially change from sample to sample and be dependent on process parameters like the firing peak temperature as well as material parameters such as dislocation density and impurity concentrations which would vary from wafer to wafer in the same ingot as well as for different manufacturers. This makes finding an average optimal point challenging unless these dependencies are known. Therefore, further experiments in multiple regions and wafers would provide a better picture of the average time and temperature range which would give the best results. These further improvements can enable having cast-mono solar cells with a reduced variance in their performance characteristics. We will also investigate the lifetime stability of these processes in the final work. Further investigations will be done to find out why the mono-like regions degrade during all these treatments.

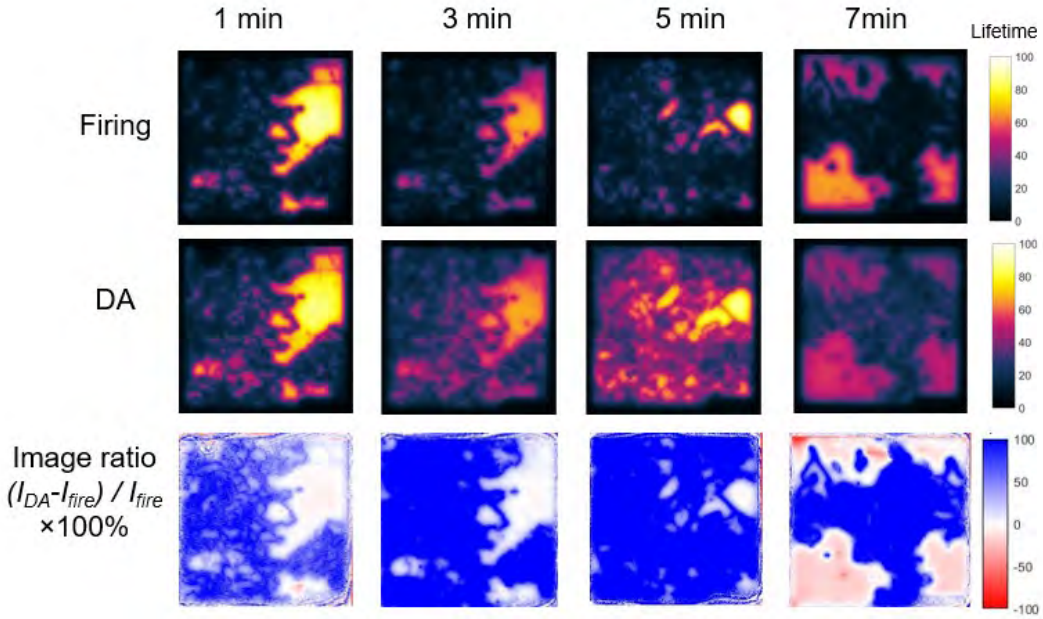

Figure 3. Calibrated lifetime PL images of the lifetime samples before and after dark annealing at different time lengths at a temperature of 300°C. The non-sister tokens could influence the final result.

References

[1] I. Guerrero *et al.*, "About the origin of low wafer performance and crystal defect generation on seed-cast growth of industrial mono-like silicon ingots," *Prog. Photovoltaics Res. Appl.*, vol. 22, no. 8, pp. 923–932, Aug. 2014.

[2] K. Jiptner, M. Fukuzawa, Y. Miyamura, H. Harada, K. Kakimoto, and T. Sekiguchi, "Evaluation of residual strain in directional solidified mono-Si ingots," *Phys. status solidi*, vol. 10, no. 1, pp. 141–145, Jan. 2013.

[3] B. Gao, S. Nakano, and K. Kakimoto, "Influence of Back-Diffusion of Iron Impurity on Lifetime Distribution near the Seed-Crystal Interface in Seed Cast-Grown Monocrystalline Silicon by Numerical Modeling," *Cryst. Growth Des.*, vol. 12, no. 1, pp. 522–525, Jan. 2012.

[4] C. Schwab *et al.*, "Evaluation of cast mono silicon material for thermal oxide passivated solar cells," *Energy Procedia*, vol. 38, pp. 611–617, 2013.

[5] X. Zhang, L. Gong, B. Wu, M. Zhou, and B. Dai, "Characteristics and value enhancement of cast silicon ingots," *Sol. Energy Mater. Sol. Cells*, vol. 139, pp. 27–33, Aug. 2015.

[6] T. Kaden *et al.*, "Analysis of Mono-cast Silicon Wafers and Solar Cells on Industrial Scale," *Energy Procedia*, vol. 27, no. April, pp. 103–108, 2012.

[7] B. J. Hallam *et al.*, "Advanced Hydrogenation of Dislocation Clusters and Boron-oxygen Defects in Silicon Solar Cells," *Energy Procedia*, vol. 77, no. February 2016, pp. 799–809, 2015.

[8] A. Samadi *et al.*, "Hydrogenation of Dislocations in p-type Cast-Mono Silicon," in *SiliconPV*, 2019.

[9] C. Dubé and J. I. Hanoka, "Hydrogen passivation of dislocations in silicon," *Appl. Phys. Lett.*, vol. 45, no. 10, pp. 1135–1137, 1984.